

## SUPPORTING INFORMATION

### Investigation of binding of UDP-Galp and UDP-[3-F]Galp to UDP-galactopyranose mutase by STD-NMR spectroscopy, molecular dynamics, and CORCEMA-ST calculations

*Yue Yuan<sup>‡</sup>, Dustin W. Bleile<sup>‡</sup>, Xin Wen<sup>†</sup>, David A. R. Sanders<sup>¶</sup>, Kenji Itoh<sup>§</sup>, Hung-wen Liu<sup>§</sup> and B. Mario Pinto<sup>‡\*</sup>*

<sup>‡</sup>Department of Chemistry, Simon Fraser University, Burnaby, British Columbia, Canada V5A 1S6

<sup>†</sup>Institute of Elemento-organic Chemistry and Department of Chemical Biology, Nankai University, Tianjin 300071, China

<sup>¶</sup>Department of Chemistry, University of Saskatchewan, 110 Science Place, Saskatoon, Saskatchewan, Canada S7N 5C9

<sup>§</sup>Division of Medicinal Chemistry, College of Pharmacy, and Department of Chemistry and Biochemistry, University of Texas, Austin, TX 78712, USA

\* Address correspondence to B. Mario Pinto, Department of Chemistry, Simon Fraser University, Burnaby, British Columbia, Canada V5A 1S6. Tel: 778-782-4152; Fax: 771-782-4860; E-mail: [bpinto@sfu.ca](mailto:bpinto@sfu.ca).

**FUNDING** This work was supported by Discovery Grants administered by the Natural Sciences and Engineering Research Council of Canada to both BMP and DARS, and a grant from the National Institutes of Health (GM54346) to HWL.

**RUNNING TITLE** Ligand Binding to UDP-Galp Mutase by STD-NMR/Modeling

**KEYWORDS** UDP-galactopyranose mutase, UDP-galactopyranose, UDP-galactofuranose, UDP-[3-F]galactofuranose, STD-NMR, CORCEMA-ST, GROMACS, AutoDock 3.0.5

**Figure 1s.** STD build-up curves for the protons in (A) UDP-Galf and (B) UDP-[3-F]Gal with different T1 times. Experimental data were fit to a rising exponential.

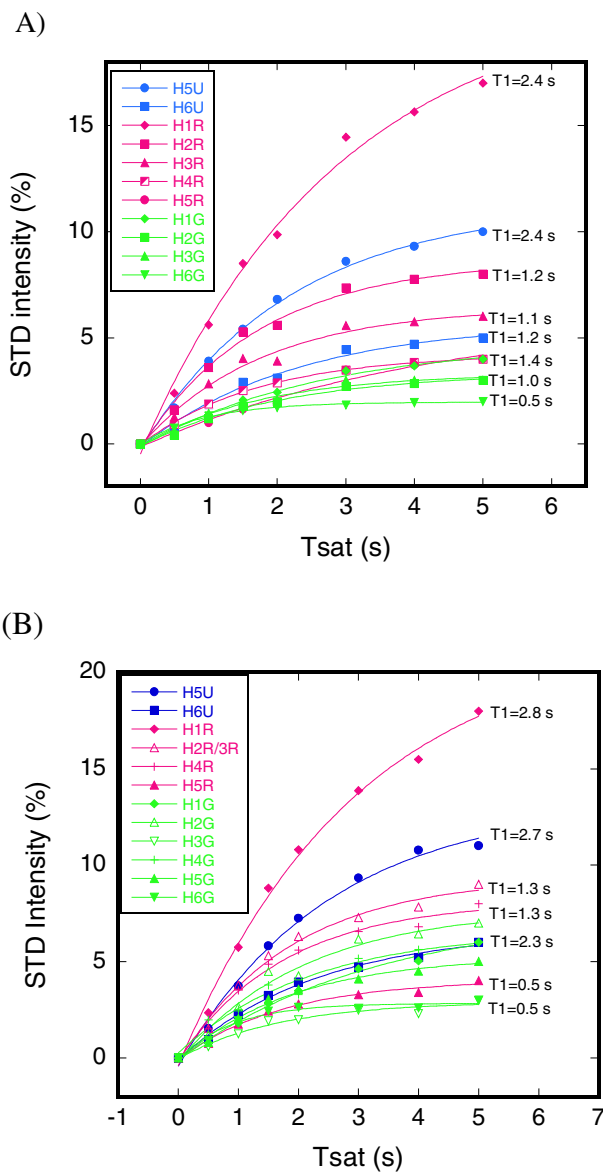


**Figure 2s.** Expansions of the 1D  $^1\text{H}$  NMR spectra of UDP-[3-F]Gal $\beta$  4 in the presence of UGM at 600 MHz at 280 K without water suppression (U: Uracil; R: Ribose; G: 3-Fluorine substituted Galactofuranose). (A) before the addition of 20 mM  $\text{Na}_2\text{S}_2\text{O}_4$ ; (B), (C) and (D) after the addition of 20 mM  $\text{Na}_2\text{S}_2\text{O}_4$  at 5, 10 and 20 minutes, respectively.

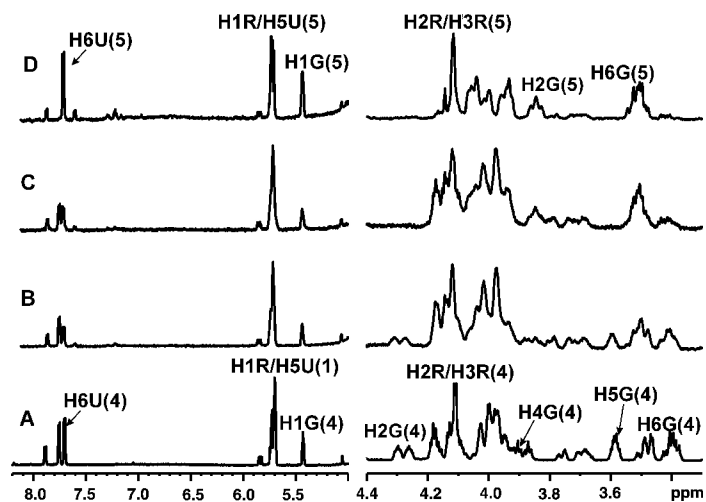
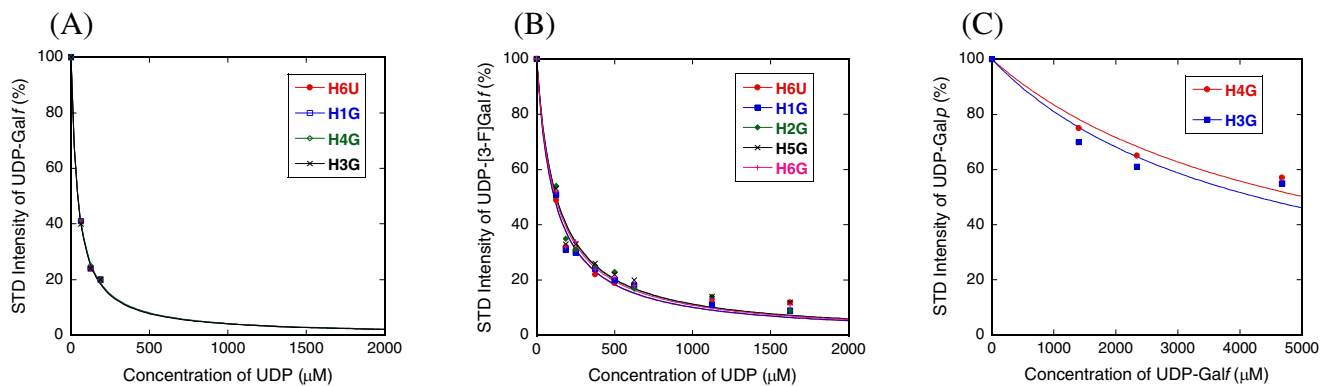


**Figure 3s.** Titration curves showing the competition binding of (A) UDP-Galf **1** with UDP **3** (B) UDP-[3-F]Galf **4** with UDP **3** to oxidized UGM. (C) Titration curve showing the competition binding of UDP-Galf **1** with UDP-Galp**2** at 5 mM concentration in the presence of oxidized UGM.



Titration curves were fitted using KaleidaGraph by eq. (1) (1, 2):

$$I_{STD} = -100 \times I_0 / (I_0 + IC_{50}) + 100 \quad \text{eq. (1)}$$

with  $I_0$  being the total concentration of UDP **3** or UDP-Galf **1**. The  $K_D$  values of **1** and **3** can be calculated based on the eq. (2) (3):

$$K_D = L_0 \times K_I / (IC_{50} - K_I) \quad \text{eq. (2)}$$

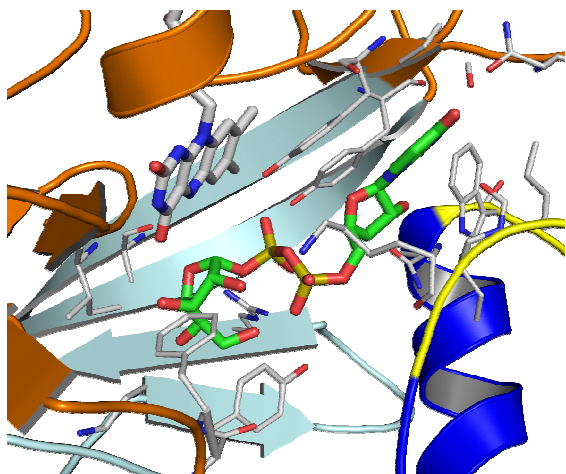
In (A) and (B),  $L_0$ , the concentration of UDP-Galf **1** and UDP-[3-F]Galf **4**, was 400 μM and 1500 μM, respectively. A range of  $IC_{50}$  values of UDP **3** was roughly 50 to 150 μM from the curve fitting. For UDP **3**, the  $K_I$  value was determined by fluorescence to be 28 μM (4). With a range of  $IC_{50}$  from 50 to 150 μM one obtains an estimate for  $K_D$  of **1** and **4** to be 400 - 800 μM.

In (C),  $IC_{50}$  of UDP-Galf **1** was in the range of 4.2 to 5.0 mM.  $L_0$ , the concentration of UDP-Galp **1**, was 5 mM, which suggested that  $K_D$  of UDP-Galf **1** and UDP-Galp**2** could be in the same range .

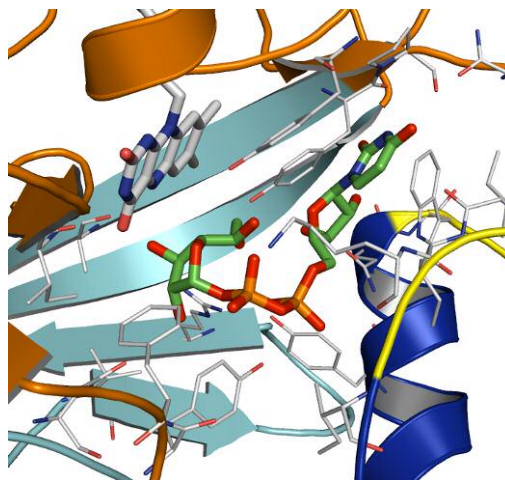


**Figure 4s.** Two binding modes observed for (A),(B) UDP-Galf **1** and (C),(D) UDP-[3-F]Galf **4** in the putative active site of UGM from AutoDock calculations. Domain 1 is colored orange; domain 2, blue; and domain 3, cyan. The two flexible loops are colored yellow. FAD, the relevant side-chains, compounds **1** and **4** are in sticks (red, oxygen; blue, nitrogen; orange, phosphate; white, carbon for FAD and the relevant side-chains; green, carbon for UDP-Galf **1** and UDP-[3-F]Galf **4**). The image was produced with PyMol (DeLano Scientific LLC) using PDB entry 1I8T.

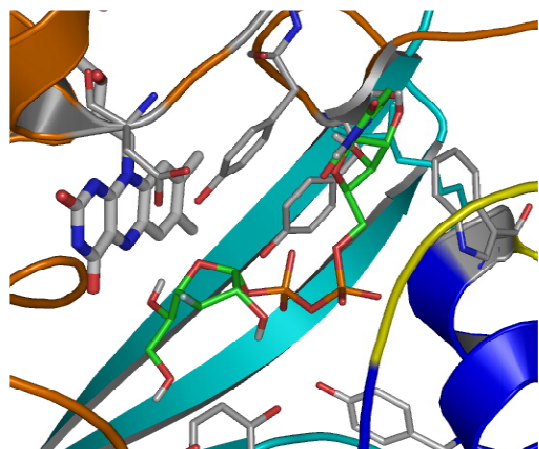
A) Conformation A of UDP-Galf **1**



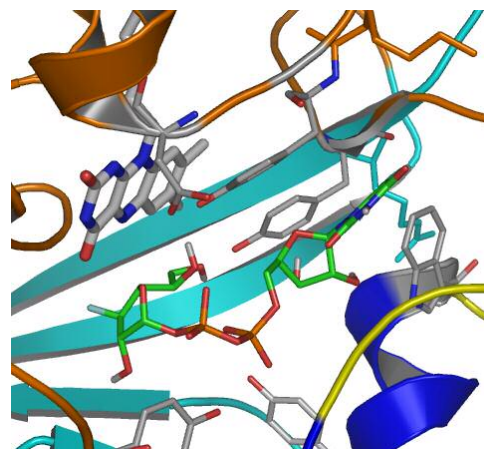
B) Conformation B of UDP-Galf **1**



C) Conformation A of UDP-[3-F]Galf **4**



D) Conformation B of UDP-[3-F]Galf **4**



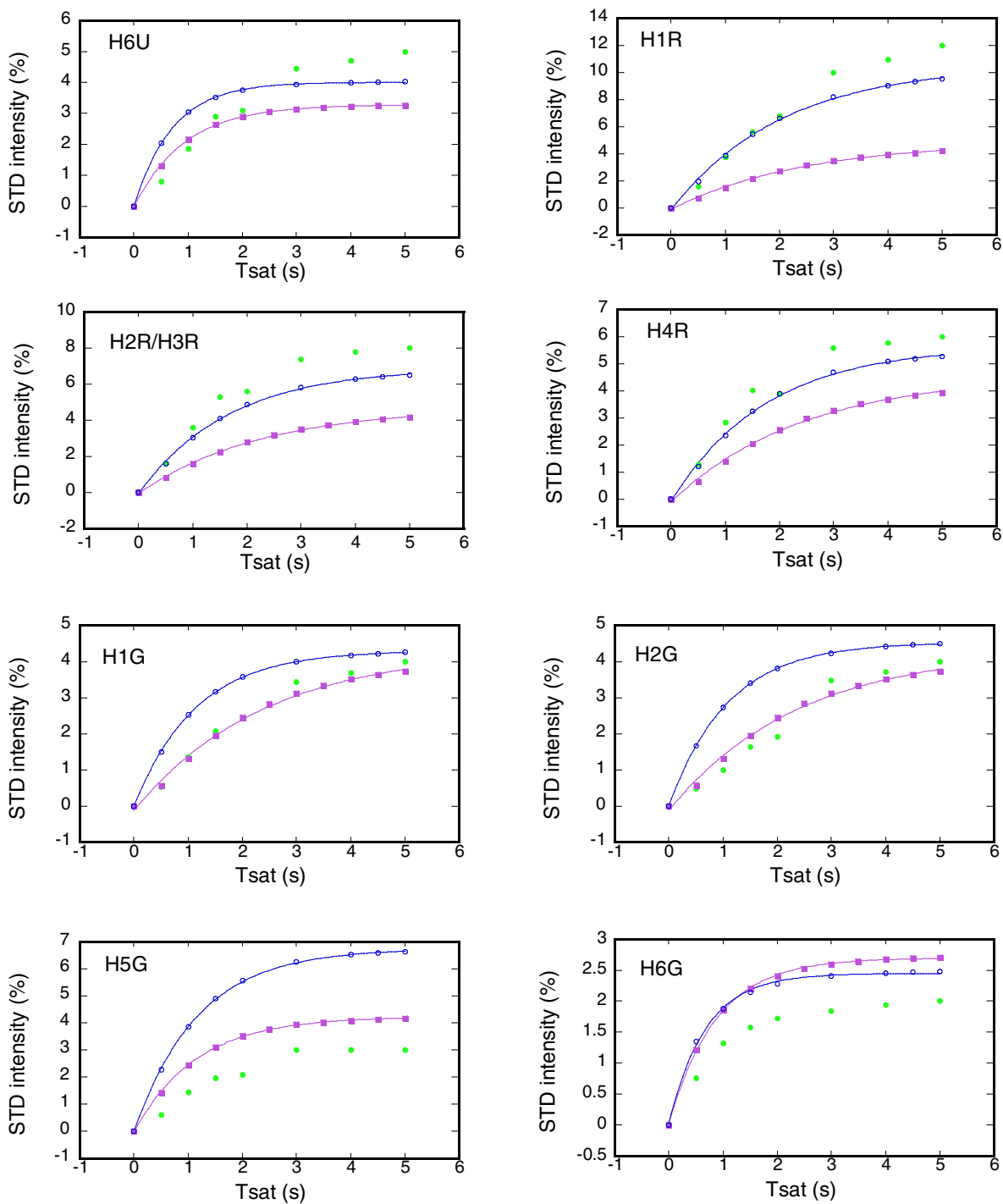
*Docked binding modes of UDP-Galf 1 and UDP-[3-F]Galf 4 in the active site of UGM.*

UDP-Galf **1** and UDP-[3-F]Galf **4** docking in the putative active site of UGM was performed with AutoDock 3.0.5 (5) as described previously (6). Considering the flexibility of the five-membered ring systems, the conformational properties of the galactofuranose moiety of **1** were studied with a random search routine (7), as implemented in Sybyl 6.6 (Tripos, Inc.) and by constraining the structure of the uridine moiety of **1**, as follows: the maximum number of search iterations was set to 3000, with a 3 kcal/mol energy cutoff, and 0.2 RMS threshold. Docking consisted of six tasks with the six different conformers of **1**, obtained from conformational analysis, representing 6 conformations of the galactofuranose moieties. All fifteen active torsions of **1** and **4** were selected to be fully flexible during the docking experiment with AutoDock 3.0.5 (5). The grid maps were constructed using  $70 \times 70 \times 70$  points, with grid point spacing of 0.375 Å. The Lamarckian Genetic Algorithm (LGA) was used with the default settings, and 500 LGA docking runs were performed for each starting structure. The results for all six tasks were combined and analyzed for a total of 3000 runs.

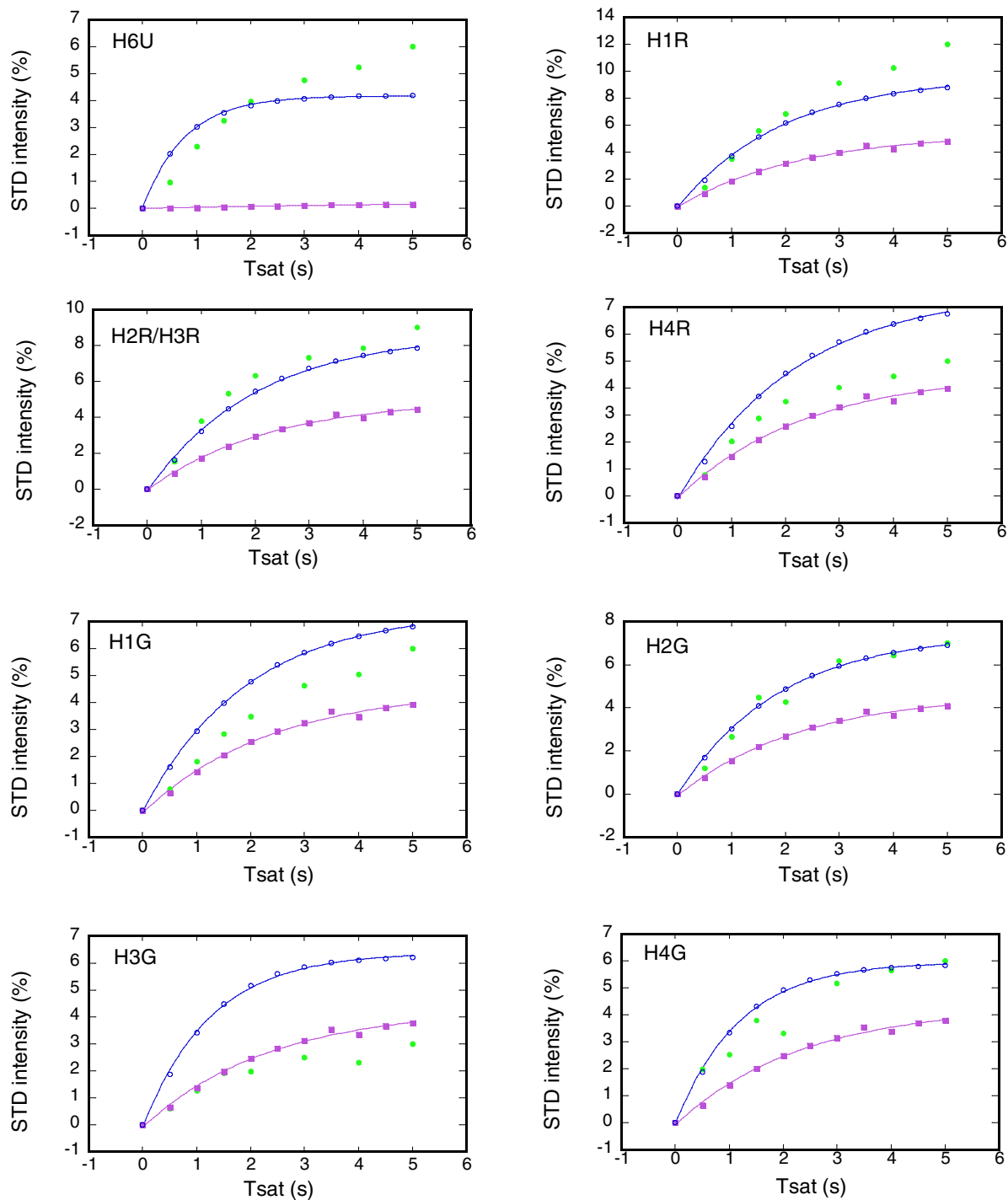
The binding modes of UDP-Galf **1** and UDP-[3-F]Galf **4** in the active site of UGM were generated by use of the AutoDock 3.0.5 program. The lowest docked energy for UDP-Galf **1** and UDP-[3-F]Galf **4**, the average energy of the first 20 clusters, together with the number of structures in each cluster, are listed in Supporting information Table 1. The resulting structures were ranked in order of increasing energy and sorted into clusters using a 2.0 Å tolerance all-atom root mean square deviation (RMSD) from the lowest energy structure. The lowest-energy docked structure of UDP-Galf **1** (Supporting information Figure 4A), with an energy of -16.19 kcal/mol, does dock in the active site of UGM, and close to the position occupied by UDP-Galp **2** shown in our previous study (8). Furthermore, the Galf moiety of this conformer (Conformation A) displayed a very similar binding mode to that of UDP-Galp **2** in UGM, which is close to the N5 atom of the flavin moiety in UGM (the distance between C1 of **1** and N5 of flavin is 3.4 Å), consistent with the proposed enzyme mechanism. However, in the same lowest-energy cluster, some galactofuranose moieties of UDP-Galf **1** appeared in an alternative orientation (Conformation B) (Supporting information Figure 4B), which was inverted relative to the Galp moiety in UDP-Galp **2**. Thus, C1 of the Galf residue was located away from the N5 atom of the flavin moiety in UGM (the distance between C1 of **1** and N5 of flavin is 5.02 Å).

The two binding modes of the UGM-**1** complex served as starting points for the docking of the fluorinated analogue UDP-[3-F]Galf **4**. Upon docking in the active site of UGM, irrespective of the binding mode chosen as a starting point, two different orientations (conformations A and B) of the Galf moiety were displayed in the lowest-energy clusters (Supporting information Figure 4C, D). The interactions between the uracil moiety with aromatic residues were also present.

**Figure 5s.** (A). Comparison of experimental (green) and predicted STD values from the CORCEMA-ST protocol for two binding models A (blue) and B (magenta) of UDP-Galf **1** in the presence of UGM. (U:Uracil; R:Ribose; G: Galactofuranose).



(B). Comparison of experimental (green) and predicted STD values from the CORCEMA-ST protocol for two binding models A (blue) and B (magenta) of UDP-[3-F]Gal $\beta$  1 in the presence of UGM. (U:Uracil; R:Ribose; G: Galactofuranose).



Theoretical STD values (blue and magenta) were predicted by the CORCEMA-ST protocol based on the binding modes of UDP-Galf **1** and UDP-[3-F]Galf **4** generated from MD simulations. The number of protons in UDP-Galf **1** and the protons of the amino acid residues within the UGM binding site, the number of protein protons that experience direct RF irradiation, and their identities were read into the program. To speed up the computation of the matrix, spectral densities were calculated for only those proton pairs having a distance of 6 Å or less. In the calculations, UDP-Galf **1** or UDP-[3-F]Galf **4** and the 26 amino acid residues within the binding pocket were included. The order parameter  $S^2$  was set to 0.25 for the methyl group while for methyl-X relaxation  $S^2$  was generally kept at 0.85. For Tyr and Phe, a simple  $\langle 1/r^6 \rangle$  average was used for the dipolar relaxation between the aromatic and other protons. The calculations were performed using the following parameters,  $S^2 = 0.25$  for the methyl group,  $S^2 = 0.85$  for methyl-X relaxation; the concentration of ligand was 2 mM and the ratio of ligand: protein was 100:1;  $k_{on} = 10^5$ ;  $K_D = 100 \mu\text{M}$ ;  $\tau = 0.5$  ns and 70 ns for ligand in free and bound states, respectively. Since the protein signals at -1.0 ppm were irradiated for the STD experiment, we made the reasonable assumption that the methyl protons in Thr, Ile, Ala, Leu, Val and FAD were instantaneously saturated, and that magnetization would take a finite time to spread to other protein and ligand protons (bound and free) through dipolar networks and chemical exchange. STD values were calculated as  $[(I_{0(k)} - I(t)_{(k)})/I_{0(k)}] \times 100$ , with  $I_{0(k)}$  being the intensity of the signal of proton  $k$  without saturation transfer at time  $t=0$ , and  $I(t)_{(k)}$  being the intensity of proton  $k$  after saturation transfer during the saturation time  $t$ . For the comparison to the experimental STD values, an NOE  $R$ -factor is defined as (9) :

$$\text{R-factor} = \sqrt{\frac{\sum (S_{\text{expt},k} - S_{\text{calc},k})^2}{\sum (S_{\text{expt},k})^2}}$$

In these equations,  $S_{\text{expt},k}$  and  $S_{\text{calc},k}$  refer to experimental and calculated STD values for proton  $k$ .

**Table 1s.** Calculated energies of UDP-Galf **1** and UDP-[3-F]Galf **4** docked in the active site of UGM.

UDP-Galf <b>1</b>			UDP-[3-F]Galf <b>4</b>		
Cluster rank <sup>a</sup>	Docked energy (kcal mol <sup>-1</sup> )	Mean docked energy (kcal mol <sup>-1</sup> )	Cluster rank <sup>a</sup>	Docked energy (kcal mol <sup>-1</sup> )	Mean docked energy (kcal mol <sup>-1</sup> )
1(30)	-16.19	-13.14	1(42)	-18.37	-9.40
2(5)	-15.09	-10.22	2(5)	-15.26	-11.59
3(25)	-14.30	-12.21	3(23)	-14.71	-10.98
4(4)	-13.96	-10.99	4(31)	-14.39	-11.07
5(1)	-13.86	-13.86	5(6)	-14.32	-10.19
6(12)	-13.63	-11.12	6(8)	-14.31	-9.09
7(12)	-13.51	-10.94	7(4)	-14.13	-11.76
8(7)	-13.40	-11.21	8(3)	-13.55	-7.35
9(2)	-13.28	-12.51	9(9)	-13.33	-9.85
10(10)	-12.83	-11.18	10(13)	-13.23	-9.58
11(8)	-12.74	-11.68	11(6)	-13.14	-11.48
12(16)	-12.52	-10.91	12(5)	-12.68	-10.61
13(5)	-12.51	-10.98	13(5)	-12.41	-9.89
14(5)	-12.42	-10.49	14(5)	-12.40	-9.66
15(3)	-12.36	-11.44	15(6)	-12.28	-9.96
16(9)	-12.30	-11.39	16(4)	-12.18	-10.66
17(1)	-12.25	-12.25	17(3)	-11.95	-9.82
18(2)	-12.08	-11.29	18(3)	-11.85	-9.77
19(9)	-12.02	-10.96	19(3)	-11.76	-10.93
20(5)	-12.00	-11.34	20(4)	-11.61	-9.30

<sup>a</sup> Number in cluster is given in parentheses.

## References

1. Benie, A. J., Moser, R., Bauml, E., Blaas, D., and Peters, T. (2003) Virus-ligand interactions: Identification and characterization of ligand binding by NMR spectroscopy, *Journal of the American Chemical Society* 125, 14-15.
2. Mayer, M., and Meyer, B. (2001) Group epitope mapping by saturation transfer difference NMR to identify segments of a ligand in direct contact with a protein receptor, *Journal of the American Chemical Society* 123, 6108-6117.
3. Cheng, Y., and Prusoff, W. H. (1973) Relationship between Inhibition Constant (K1) and Concentration of Inhibitor Which Causes 50 Per Cent Inhibition (I50) of an Enzymatic-Reaction, *Biochemical Pharmacology* 22, 3099-3108.
4. Yao, X., Bleile, D. W., Yuan, Y., Cho, J., Sarathy, K. P., Sanders, D. A. R., Pinto, B. M., and O'Neill, M. A. (2007) Substrate Regulates Redox-Switched Recognition Loop Dynamics in UDP-Galactopyranose Mutase, *unpublished results*.
5. Morris, G. M., Goodsell, D. S., Halliday, R. S., Huey, R., Hart, W. E., Belew, R. K., and Olson, A. J. (1998) Automated docking using a Lamarckian genetic algorithm and an empirical binding free energy function, *Journal of Computational Chemistry* 19, 1639-1662.
6. Yuan, Y., Wen, X., Sanders, D. A. R., and Pinto, B. M. (2005) Exploring the mechanism of binding of UDP-galactopyranose to UDP-galactopyranose mutase by STD-NMR spectroscopy and molecular modeling, *Biochemistry* 44, 14080-14089.
7. Saunders, M., Houk, K. N., Wu, Y. D., Still, W. C., Lipton, M., Chang, G., and Guida, W. C. (1990) Conformations of Cycloheptadecane - a Comparison of Methods for Conformational Searching, *Journal of the American Chemical Society* 112, 1419-1427.
8. Sanders, D. A. R., Staines, A. G., McMahon, S. A., McNeil, M. R., Whitfield, C., and Naismith, J. H. (2001) UDP-galactopyranose mutase has a novel structure and mechanism, *Nature Structural Biology* 8, 858-863.
9. Rama Krishna, N., and Jayalakshmi, V. (2006) Complete relaxation and conformational exchange matrix analysis of STD-NMR spectra of ligand-receptor complexes, *Progress in Nuclear Magnetic Resonance Spectroscopy* 49, 1-25.